PHYSICAL REVIEW A, VOLUME 63, 031801(R)

Strong parametric amplification by spatial soliton-induced cloning of transverse beam profiles in an all-optical antiwaveguide

D. Bortman-Arbiv, A. D. Wilson-Gordon, and H. Friedmann
Department of Chemistry, Bar-Ilan University, Ramat Gan 52900, Israel
(Received 6 September 2000; published 7 February 2001)

Spatial soliton-induced cloning, which achieves and maintains perfect spatial overlap of interacting beams, is proposed as a tool for amplification of nonlinear optical effects on propagation. This is illustrated by the enhancement of the parametric amplification, obtained through pump-induced cloning of the transverse profiles of the copropagating probe and generated four-wave mixing beams, in an all-optical antiwaveguiding configuration.

DOI: 10.1103/PhysRevA.63.031801   PACS number(s): 42.65.Sf, 42.65.Tg, 42.65.Wi

Spatial soliton-induced *cloning*, which achieves and maintains perfect, spatial overlap of interacting light beams, is proposed as an alternative method for strong enhancement of nonlinear optical effects on propagation. The specific conditions under which this method can be implemented will be analyzed for a particular case. We consider the enhancement of parametric amplification (PA) resulting from the pump-induced cloning of the transverse profiles of a weak probe, and of the generated four-wave mixing (FWM) beam, for the case where the pump has a doughnut-shaped transverse profile [1]. The waist size of the Gaussian transverse profile of the input probe beam is chosen to be much smaller than that of the Laguerre-Gaussian pump so that, initially, there is no overlap of the beams. The beams propagate coaxially in a medium of two-level atoms. Due to self-focusing and diffraction, the pump beam is transformed into a bright vortex, or doughnut, spatial soliton [2]. Cloning arises from diffraction and sufficiently strong pump-induced focusing [3] of the probe and of the generated FWM beam, and leads to enhanced PA of both beams on propagation. We have verified that in an alternative scenario, where the pump-induced focusing of the probe is weaker, the probe intensity still leaves the region of the propagation axis and concentrates in the bright region of the pump. However, the overlap between the pump and probe beams is less perfect, leading at first to weak PA. On further propagation, PA increases the probe and FWM intensity and this eventually leads to cloning since PA is controlled by the pump. Thus PA seems to reinforce the effect of cross-focusing [4] and reduces the anticloning tendency of diffraction, thereby playing a self-referential role.

Amplification depends on the propagation distance and therefore transverse instability, leading to breakup of the bright vortex soliton, must be suppressed. This is achieved by working under saturation conditions [2] and using computer-generated holograms rather than a cylindrical lens mode converter to prepare the Laguerre-Gaussian beam [1,5]. In this way, one can avoid azimuthal-symmetry-breaking perturbations that introduce ellipticity into the transverse profile [2]. In computer simulations, azimuthal symmetry breaking is avoided by using a polar grid that prevents the numerical noise effects of discretizing a ring onto a rectangular grid [2]. Thus the transverse field keeps its initial azimuthal symmetry so that a cylindrical two-dimensional numerical method can be used to calculate the beam propagation [6].

Cloning has been discussed by Vemuri *et al.* [7] in a different context where a strong 2π pump soliton confers its soliton property on a weak probe pulse, by amplification due to the stimulated Stokes Raman effect, in a resonant Λ system. In contrast to our scheme, the transverse profiles and diffraction were not considered and spatial overlap of the input pulses was implicit.

Recently, electromagnetically induced waveguiding in atomic rubidium has been demonstrated both experimentally [1] and theoretically [8]. The atom was modeled as a V system. Waveguiding was achieved by the interaction of an intense pump with a Laguerre-Gaussian charge 3 profile, creating a transverse refractive-index profile for the probe, similar to that of a conventional optical fiber. Amplification does not take place in such a configuration.

As opposed to induced waveguiding where the weak beam is guided along the propagation axis, we focus on the effect of *antiwaveguiding* and its potential applications. Antiwaveguides are structures where the beam is guided out of the core area and into the cladding. In fiber antiwaveguides, the linear refractive index of the core is less than that of the cladding, in contrast to the more common waveguides where the opposite situation obtains. Gisin *et al.* [9] found, by numerically calculating the eigenvalues of the Schrödinger equation with a ''potential hill,'' that antiwaveguides support stable solutions localized near the core. They also showed [10] that antiwaveguides may be used to obtain second-harmonic generation.

Here, an *all-optical antiwaveguide* for a weak probe is created by the copropagating Laguerre-Gaussian charge 3 pump beam [1,8]. This optically induced antiwaveguiding scheme generates several effects, arising from the interaction of the two incident beams and the weak beam generated by FWM, in the presence of diffraction. These are (i) the antiwaveguiding of the probe, (ii) the reshaping of the transverse profile of the probe from its initial Gaussian form into a clone of the pump profile, (iii) the appearance of a new weak beam at the FWM frequency whose azimuthal phase is twice that of the pump beam [11–13] and whose transverse profile is a clone of the pump, and (iv) enhanced PA of both clones on propagation due to the overlap of the interacting beams. It should be stressed that cloning is not achieved trivially since in the case of weak cross-focusing, the probe will spread out due to diffraction, decreasing PA. To our knowledge, the spatial-soliton induced cloning of transverse beam profiles, and its role in the amplification of nonlinear processes, has not been discussed before for atomic systems. Note, however, that Lundquist *et al.* [14] have discussed the creation of a three-color spatial soliton by the interaction between a beam at the central frequency and two sideband waves, through cross-phase modulation and parametric FWM, in a two-dimensional Kerr medium.

We consider the interaction between an incident cw electromagnetic field of the form $\tilde{\mathbf{E}}(\mathbf{r},t)=\Sigma_{Q=L,P}\tilde{\mathbf{E}}_Q(\mathbf{r},t)=\Sigma_{Q=L,P}\mathbf{E}_Q(\mathbf{r})e^{-i(\omega_Q t-\mathbf{k}_Q\cdot\mathbf{r})}+\text{c.c.}$ and a medium consisting of two-level atoms with lower state $|a\rangle$, upper state $|b\rangle$, and transition frequency ω_{ba}. $\mathbf{E}_L(\mathbf{r})$ and $\mathbf{E}_P(\mathbf{r})$ represent the slowly varying envelope amplitude of the strong pump field and the weak probe field, respectively, and ω_L and ω_P are the pump and probe frequencies with wave vectors $\mathbf{k}_L$ and $\mathbf{k}_P$. The two incident laser beams propagate in the z direction through the atomic medium. The dynamics of these two beams and of the generated FWM beam, $\tilde{\mathbf{E}}_M(\mathbf{r},\mathbf{t})=\mathbf{E}_M(\mathbf{r})e^{-i(\omega_M t-\mathbf{k}_M\cdot\mathbf{r})}+\text{c.c.}$ at frequency $\omega_M=2\omega_L-\omega_P$ and wave vector $\mathbf{k}_M$, is determined by solving the coupled Maxwell-Bloch equations [15,16]

$$-\nabla^2\tilde{\mathbf{E}}_J(\mathbf{r},t)+\frac{1}{c^2}\frac{\partial^2}{\partial t^2}\tilde{\mathbf{E}}_J(\mathbf{r},t)=-\frac{4\pi}{c^2}\frac{\partial^2}{\partial t^2}\tilde{\mathbf{P}}_J(\mathbf{r},t),\quad J=L,P,M, \tag{1}$$

where $\tilde{\mathbf{P}}_J(\mathbf{r},t)$ is the induced polarization of the medium given by $\tilde{\mathbf{P}}=N\langle\tilde{\mu}\rangle=N\langle\text{Tr}(\hat{\rho}\hat{\mu})\rangle$, N is the atomic number density, $\hat{\mu}$ is the dipole moment operator, and $\hat{\rho}$ is the density operator. The density matrix elements of this two-level system are calculated from the steady-state Bloch equations (see [16]). Assuming the paraxial approximation, the coupled amplitude equations take the form

$$\frac{\partial}{\partial z}U_L=\frac{i}{4L_D}\nabla_T^2U_L+\frac{i}{L_{NL}}\alpha_LU_L, \tag{2}$$

$$\frac{\partial}{\partial z}U_P=\frac{i}{4L_D}\nabla_T^2U_P+\frac{i}{L_{NL}}\alpha_PU_P+\frac{i}{L_{NL}}\kappa_PU_L^2U_M^*, \tag{3}$$

$$\frac{\partial}{\partial z}U_M=\frac{i}{4L_D}\nabla_T^2U_M+\frac{i}{L_{NL}}\alpha_MU_M+\frac{i}{L_{NL}}\kappa_MU_L^2U_P^*, \tag{4}$$

where $\nabla_T^2=\partial^2/\partial\xi^2+(1/\xi)\partial/\partial\xi+(1/\xi^2)\partial^2/\partial\theta^2$ is the transverse Laplacian in dimensionless cylindrical coordinates, $\xi=r/\sqrt{2}w_{0L}$. $U_J(z,\xi,\theta)=U_J(z,\xi)\exp(-ia_J\theta)$ with $a_L=3$, $a_M=2a_L=6$ (assuming azimuthal phase matching), and $a_P=0$ [17], and $U_J(z,\xi)=A_J(z,\xi)/A_{0L}$ are normalized field variables. Here A_{0L}^2 is the dimensionless peak intensity of the incident pump, $2A_J=\mu T_2E_J/\hbar$ are dimensionless pump, probe, and FWM Rabi frequencies, and T_2 is the transverse decay time. In Eqs. (2)–(4), the parameter $L_{NL}=\hbar/\pi kN\mu^2T_2$ is a characteristic length indicating the strength of the nonlinear term, $L_D=kw_{0L}^2$ is the diffraction length, and w_{0L} is the initial spot size of the pump transverse profile. The wave vector is given by $k=|\mathbf{k}_J|\simeq\omega_L/c$, and the coefficients α_J and $\kappa_{P,M}$ are given by $\alpha_J=\rho_{ba}(\omega_J)/A_J$, $\kappa_P=\rho_{ba}(\omega_P=2\omega_L-\omega_M)/A_M^*U_L^2$, and $\kappa_M=\rho_{ba}(\omega_M=2\omega_L-\omega_P)/A_P^*U_L^2$. The coefficients α_J account for self-induced absorption and refraction of the pump, and for cross-induced (pump-induced) absorption and refraction of the probe and the created FWM beam. The terms $\kappa_{P,M}$ determine the coupling strength of the parametric mixing of the weak beams U_P and U_M. These complex coefficients depend on the choice of parameters such as the detunings $\Delta_J=\omega_{ba}-\omega_J$ of the beam frequencies from the resonance frequency ω_{ba}, the rate of collisional dephasing $1/T_2$, and, via the pump Rabi frequency A_L, on the transverse coordinate ξ. The last terms of Eqs. (3) and (4) show that PA increases with increasing overlap of the probe and FWM beams with the pump.

In our previous work [18,19] on propagation in the two-level system approximation, we were mainly interested in induced waveguiding. Here, we focus on *all-optical anti-waveguiding*, where the antiwaveguiding conditions are created by the pump for the weak copropagating probe. The conditions for realizing an induced antiwaveguide are determined by the pump, probe, and FWM parameters. We have shown previously [19] that a self-focusing pump with $\Delta_L<0$ induces a probe refractive index that increases with pump intensity, for a probe whose frequency satisfies $\Delta_P=\Delta_L-\delta<0$. Thus the probe beam will be focused towards the high intensity region of the pump. Therefore, in a configuration where the probe beam has a Gaussian transverse intensity profile, whereas the pump is *concentrated* at the periphery, the pump acts as an *antiwaveguide* for probe propagation. This is achieved by choosing a pump beam, whose transverse intensity profile is Laguerre-Gaussian, and a coaxial Gaussian probe beam. Similarly, the FWM beam will be focused towards the high intensity region of the pump if $\Delta_M=\Delta_L+\delta<0$. Thus the general condition for achieving antiwaveguiding is $\Delta_J<0$, which implies that $|\delta|<|\Delta_L|$. Reshaping due to absorption of the pump is mini-

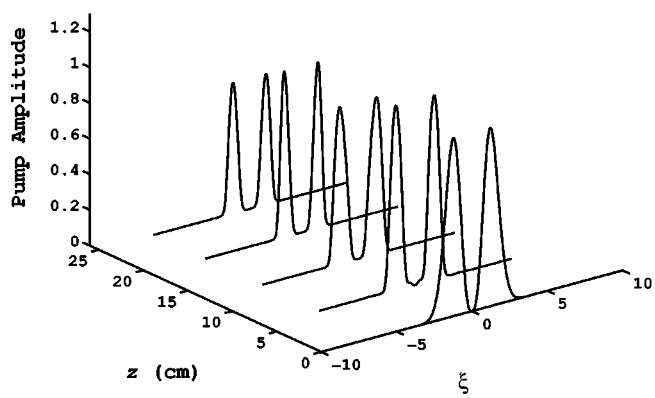

FIG. 1. The transverse amplitude profile of the pump, as a function of ξ for various values of propagation length z. The pump amplitude is initially normalized to unity. The parameters are $A_{0L}=50$, $\Delta_LT_2=-30$, $T_2=0.1T_1$, $L_D=1.5$ cm, and $L_{NL}=1\times10^{-3}$ cm.

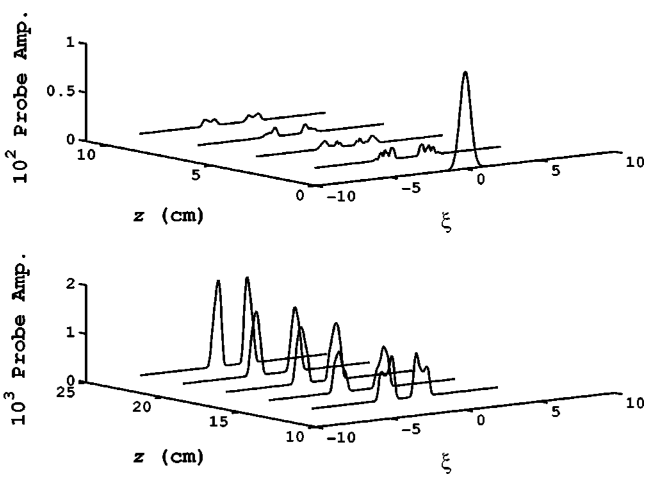

FIG. 2. The transverse amplitude profile of the probe copropagating with a pump, as a function of ξ for various values of propagation length z. The probe amplitude is relative to the initial amplitude of the pump. The parameters are $A_{0L}=50$, $A_{0P}=10^{-2}A_{0L}$, $\Delta_L T_2=-30$, $\delta T_2=-20$, $T_2=0.1T_1$, $L_D=1.5$ cm, and $L_{NL}=1\times10^{-3}$ cm.

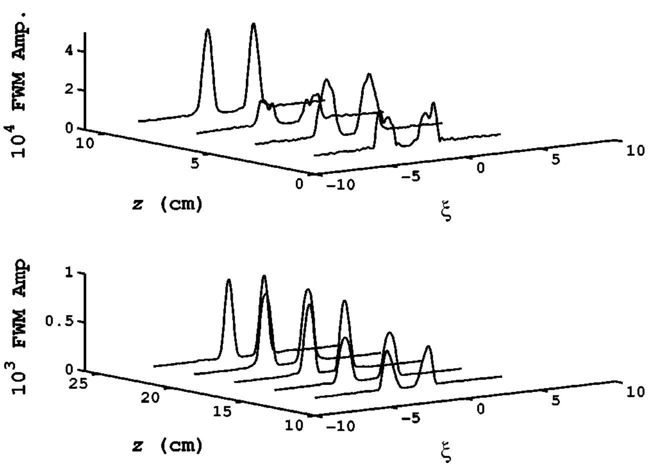

FIG. 3. The transverse amplitude profile of the FWM beam, as a function of the propagation distance z. The FWM amplitude is relative to the initial amplitude of the pump. The parameters are the same as in Fig. 2.

mized by choosing a large detuning $|\Delta_L|\gg 1/T_2$ and by introducing dephasing collisions that decrease T_2 and hence the value of $\mathrm{Im}\,\alpha_L$. The effect of Doppler broadening is negligible for this system, since the detunings are much larger than typical values of the Doppler width.

For numerical simulations, we use a Laguerre-Gaussian charge 3 doughnut beam, as in the waveguiding experiment of Truscott *et al.* [1], and a Gaussian probe,

$$U_L(\xi,\theta,z=0)=\xi^3\exp(-\xi^2)\exp(-3i\theta), \tag{5}$$

$$U_P(\xi,z=0)=(A_{0P}/A_{0L})\exp[-\xi^2(w_{0L}^2/w_{0P}^2)]. \tag{6}$$

We solve Eqs. (2)–(4) numerically by a procedure based on the discretization of the transverse Laplacian in terms of second-order differences and the integration of the first-order differential equations by the fourth-order Runge-Kutta method.

In the results presented here, the pump is detuned to the high-frequency side of the atomic resonance with $\Delta_L T_2=-30$, the pump-probe detuning is $\delta T_2=-20$, and $T_2=0.1\ T_1$. The initial dimensionless pump and probe Rabi frequencies are $2A_{0L}=100$ and $A_{0P}=10^{-2}A_{0L}$. The waist size of the probe is initially $w_{0P}=0.5w_{0L}$, so that almost all the probe beam is contained in the region where the pump intensity is almost zero. The nonlinear and diffraction lengths are $L_{NL}=1\times10^{-3}$ cm and $L_D=1.5$cm. In Fig. 1 we show the transverse amplitude profile of the pump as a function of the propagation distance up to 25 cm. On propagation, the transverse amplitude profile of the pump focuses slightly towards its high intensity region, due to the effect of self-focusing. For the parameters chosen, the effects of diffraction and self-focusing are nearly balanced and the pump profile transverse profile does not change significantly during propagation. We now turn to the propagation of the probe as shown in Fig. 2. The initially narrow Gaussian probe is rapidly guided away from the center towards the periphery, due to the combined effects of absorption and defocusing induced by the pump near the axis. The resulting probe profile has a doughnut shape with oscillatory structure at the high intensity periphery. After a propagation distance of almost 10 cm, the modified probe beam gradually becomes smooth and assumes the same form as the pump. Thus, the initially Gaussian probe is reshaped so that its intensity becomes centered at the periphery. On further propagation, the probe is enhanced by PA, due to the coupling to the weak FWM beam, which itself is created and amplified in the high intensity region of the pump (see Fig. 3).

Figures 1–3 have been calculated taking $\Delta_L T_2=-30$ and $\delta T_2=-20$ so that the probe is closer to resonance than the pump. For this choice, probe cross focusing is about five times larger than for the opposite case where $\delta T_2=20$. We have verified that, in that case, diffraction is not completely balanced by cross focusing and, consequently, antiwaveguiding is not accompanied by cloning up to a propagation distance of ~30 cm. However, the FWM beam that is generated in the high-intensity region of the pump is rapidly cloned, leading to amplification of the probe by parametric interaction. This also takes place in the high intensity region of the pump and leads eventually to cloning of the probe.

The phenomena that have been described in this work can be realized in a medium consisting of atomic vapor, for example, sodium atoms. The $3\,^2S_{1/2}-3\,^2P_{3/2}$ transition of sodium with transition wavelength $\lambda_0=589$ nm forms an effective two-level system. This system has been proposed as a possible candidate to observe phenomena such as induced spatial solitons [18], and the effect of FWM on induced waveguiding [19]. The effects of antiwaveguiding, cloning, and PA enhancement, presented here, are quite general and should also be observable in saturable Kerr media [2], in an all-optical antiwaveguiding configuration.

This research was supported by the Israel Science Foundation administered by the Israel Academy of Sciences and Humanities. We thank B. A. Malomed, M. J. Padgett, and D. V. Skryabin for advice.

[1] A. G. Truscott, M. E. J. Friese, N. R. Heckenberg, and H. Rubinsztein-Dunlop, Phys. Rev. Lett. **82**, 1438 (1999).
[2] D. V. Skryabin and W. J. Firth, Phys. Rev. E **58**, 3916 (1998).
[3] H. Friedmann and A. D. Wilson-Gordon, Opt. Commun. **116**, 163 (1995); Phys. Rev. A **52**, 4070 (1995).
[4] L. Berge, O. Bang, and W. Krolikowski, Phys. Rev. Lett. **84**, 3302 (2000).
[5] M. J. Padgett (personal communication).
[6] J. Marcou, J. L. Auguste, and J. M. Blondy, Opt. Fiber Technol.: Mater., Devices Syst. **5**, 105 (1999).
[7] G. Vemuri, G. S. Agarwal, and K. V. Vasavada, Phys. Rev. Lett. **79**, 3889 (1997).
[8] R. Kapoor and G. S. Agarwal, Phys. Rev. A **61**, 053818 (2000).
[9] B. V. Gisin and A. A. Hardy, Phys. Rev. A **48**, 3466 (1993); B. V. Gisin, A. A. Hardy, and B. A. Malomed, Phys. Rev. E **50**, 3274 (1994).
[10] B. V. Gisin, Phys. Rev. A **59**, 3120 (1999).
[11] T. J. Alexander, Y. S. Kivshar, A. V. Buryak, and R. A. Sammut, Phys. Rev. E **61**, 2042 (2000).
[12] J. Courtial, K. Dholakia, L. Allen, and M. J. Padgett, Phys. Rev. A **56**, 4193 (1997).
[13] J. W. R. Tabosa and D. V. Petrov, Phys. Rev. Lett. **83**, 4967 (1999).
[14] P. B. Lundquist, D. R. Andersen, and Y. S. Kivshar, Phys. Rev. E **57**, 3551 (1998).
[15] Robert W. Boyd, *Nonlinear Optics* (Academic Press, New York, 1992).
[16] H. Friedmann and A. D. Wilson-Gordon, Phys. Rev. A **36**, 1333 (1987).
[17] This implies that the azimuthal phase of the incident beam is not affected by propagation. This is justified, since it has been shown experimentally [1] that it is possible to avoid azimuthal symmetry breaking for a sufficiently long propagation length.
[18] D. Bortman-Arbiv, A. D. Wilson-Gordon, and H. Friedmann, Phys. Rev. A **58**, R3403 (1998).
[19] D. Bortman-Arbiv, A. D. Wilson-Gordon, and H. Friedmann, Phys. Rev. A **61**, 033806 (2000).